

# SINGLE HIGGS-BOSON PRODUCTION AT A PHOTON-PHOTON COLLIDER: GENERAL 2HDM VERSUS MSSM

David López-Val<sup>a</sup> and Joan Solà<sup>b</sup>

<sup>a</sup> *Institut für Theoretische Physik, Universität Heidelberg  
Philosophenweg 16, D-69120 Heidelberg, Germany*

<sup>b</sup> *High Energy Physics Group, Dept. ECM, and Institut de Ciències del Cosmos  
Univ. de Barcelona, Av. Diagonal 647, E-08028 Barcelona, Catalonia, Spain  
E-mails: lopez@thphys.uni-heidelberg.de, sola@ecm.ub.es.*

**Abstract.** We revisit the production of a single Higgs boson from direct  $\gamma\gamma$ -scattering at a photon collider. We compute the total cross section  $\sigma(\gamma\gamma \rightarrow h)$  (for  $h = h^0, H^0, A^0$ ), and the strength of the effective  $g_{h^0\gamma\gamma}$  coupling normalized to the Standard Model (SM), for both the general Two-Higgs-Doublet Model (2HDM) and the Minimal Supersymmetric Standard Model (MSSM). In both cases the predicted production rates for the  $\mathcal{CP}$ -even (odd) states render up to  $10^4$  ( $10^3$ ) events per  $500\text{fb}^{-1}$  of integrated luminosity, in full consistency with all the theoretical and phenomenological constraints. Depending on the channel the maximum rates can be larger or smaller than the SM expectations, but in most of the parameter space they should be well measurable. We analyze how these departures depend on the dynamics underlying each of the models, supersymmetric and non-supersymmetric, and highlight the possible distinctive phenomenological signatures. We demonstrate that this process could be extremely useful to discern non-supersymmetric Higgs bosons from supersymmetric ones. Furthermore, in the MSSM case, we show that  $\gamma\gamma$ -physics could decisively help to overcome the serious impasse afflicting Higgs boson physics at the infamous “LHC wedge”.

## 1 Introduction

Deciphering the origin of the Electroweak Symmetry Breaking (EWSB) and the generation of masses is perhaps the most pressing unsettled puzzle in the theory of Elementary Particles. The Higgs (Englert-Brout and Guralnik-Hagen-Kibble) mechanism [1] endows the Standard Model (SM) of Strong and Electroweak interactions with an elegant answer, at the expense of introducing a new (and so far unobserved) neutral, spinless, fundamental degree of freedom. The discovery of the Higgs boson, and the study of its phenomenological features, ranks very high in the wish list of the experimental program currently underway at the Tevatron and the LHC [2]. Beyond its simplest description embodied by the SM, the phenomenon of EWSB can originate from a more complicated structure entailing a larger spectrum of Higgs bosons and a richer pattern of interactions. The general Two-Higgs-Doublet Model (2HDM) [3, 4] is a trademark example of the latter, and it is realized, in particular, by the Higgs sector of the Minimal Supersymmetric Standard Model (MSSM) [5]. Should the Higgs mechanism be the option actually chosen by Nature, it would then be mandatory to experimentally settle not only the quantum numbers and mass spectrum of the Higgs boson(s), but also the entire dynamics of the sector: namely, the gauge couplings of the Higgs bosons, their Yukawa couplings to the quarks and leptons and their own self-interactions.

In this endeavor, the future TeV-range Linear Colliders can play a key role as complementary tool to the currently ongoing hadronic machines [6].

As stressed repeatedly in the literature, one particularly interesting running mode of a linac facility is the real  $\gamma\gamma$  mode [7]. While the basic operation setup for linear colliders is the head-on scattering of high energetic electrons/positron beams, a very compelling alternative consists in transforming such  $e^+e^-$  facility into a photon-photon (or eventually an electron-photon) machine through Compton (back)-scattering of the original lepton beams with laser pulses. Among the many attractive features, photon colliders would allow to directly probe the loop-induced  $\gamma\gamma H$  coupling, which constitutes a direct handle on the quantum structure of the SM – and, in fact, of any Higgs sector extension of it, such as the general 2HDM, or the particularly interesting case of the MSSM. However, whereas the MSSM computation of  $\sigma(\gamma\gamma \rightarrow h)$  has been dealt with on several occasions in the literature since long ago [8, 9], to the best of our knowledge the first calculation of  $\sigma(\gamma\gamma \rightarrow h)$  in the general 2HDM is the one presented in Ref. [10], where the production of one single Higgs boson is addressed both from the point of view of real  $\gamma\gamma$  collisions, and also within the more traditional viewpoint of the quasi-real two-photon scattering mode at an  $e^+e^-$  collider<sup>1</sup>.

In this Letter, we revisit our original results [10] in the light of the most recent and restrictive set of constraints on the 2HDM parameter space, and we take the opportunity to closely compare the new 2HDM results with our own independent calculation of the corresponding  $\gamma\gamma \rightarrow h$  yield for the MSSM, while highlighting also the distinctive signatures in each case. It is important to understand that the enhancing mechanisms in both frameworks can be very different. While in the context of the MSSM we expect a panoply of Yukawa, and Yukawa-like, couplings of various kinds (including squark interactions with the Higgs bosons), whose phenomenological implications have been exploited in the past in a variety of important processes (see e.g. [13]), in the case of the general 2HDM we count on alternative mechanisms. Here we rely not only on the enhanced Yukawa couplings with Higgs bosons, but also on the trilinear self-interactions of the latter, whose potential effects have also been investigated in great detail in the past, as well as recently, for different processes of Higgs boson decay and production [14–17]. Worth noticing is that these enhanced trilinear interactions are not possible for the MSSM, a fact which may lead in principle to a significant distinction. However, the many restrictions imposed by perturbativity, unitarity, custodial symmetry, flavor physics, direct searches etc. may greatly subdue the overall impact of the enhancement sources in both frameworks, and it is not obvious how these processes compare to each other and whether they have realistic possibilities to be measured in the light of the present bounds. Therefore, we believe that a fully updated comparative study of the  $\gamma\gamma \rightarrow h$  mechanism in the general 2HDM versus the MSSM is timely and can be very useful to illustrate the importance of the direct  $\gamma\gamma$  collisions for the study of the Higgs boson physics.

The most remarkable conclusion of this investigation is that, despite the many theoretical and phenomenological restrictions substantially undermining the full enhancing capabilities of the new interactions beyond the SM, the  $\gamma\gamma \rightarrow h$  processes may definitely play a momentous role in the task of neatly disentangling the nature of the Higgs boson(s) potentially produced in the future TeV-class linear  $e^+e^-$  colliders running in the  $\gamma\gamma$  mode. This mode provides perhaps one the cleanest mechanisms to study Higgs boson physics in the high energy colliders.

## 2 Phenomenological and computational setup

The general 2HDM [3] follows by extending the SM Higgs sector with a second  $SU_L(2)$  doublet with weak hypercharge  $Y = +1$  and by considering the most general two-Higgs-doublet scalar field potential that one can construct compatible with  $\mathcal{CP}$ -invariance and renormalizability. Its physical

---

<sup>1</sup>See also Ref. [11] for the study of the Higgs pairwise production  $\gamma\gamma \rightarrow hh$ , and [12] for related processes.

spectrum contains two charged states,  $H^\pm$ , two neutral CP-even  $h^0, H^0$  (with masses  $M_{h^0} < M_{H^0}$ ) and one CP-odd state  $A^0$ . The structure of the 2HDM potential can eventually be expressed in terms of the masses of the physical Higgs particles ( $M_{h^0}, M_{H^0}, M_{A^0}, M_{H^\pm}$ ); the parameter  $\tan\beta$  (the ratio  $\langle H_2^0 \rangle / \langle H_1^0 \rangle$  of the two VEV's giving masses to the up- and down-like quarks); the mixing angle  $\alpha$  between the two CP-even states; and, finally, of one genuine Higgs boson self-coupling, usually denoted as  $\lambda_5$ , which cannot be expressed in terms of masses or other parameters of the model <sup>2</sup>. As for the Yukawa sector involving Higgs-quark interactions, the absence of tree-level flavor changing neutral currents (FCNC) leads to two main 2HDM scenarios: 1) type-I 2HDM, in which one Higgs doublet couples to all quarks, whereas the other doublet does not couple to them at all; 2) type-II 2HDM, where one doublet couples only to down-like quarks and the other doublet just to up-like quarks. Other flavor structures are also conceivable and have indeed attracted a growing attention in the recent years [18], but we will stick here to just the two aforementioned leading 2HDM models, which traditionally represent the two canonical options.

The very same Higgs spectrum emerges naturally from the MSSM, although SUSY constraints narrow the free parameters of the Higgs sector down to 2, usually taken to be  $\tan\beta$  and  $M_{A^0}$ . The corresponding Yukawa sector mimicks that of a type-II one, although of a very restricted sort – enforced again by SUSY invariance [3]. Most significantly, while the generic 2HDM allows triple (3H) and quartic (4H) Higgs self-interactions to be largely enhanced, in the MSSM these Higgs self-couplings are restrained to be purely gauge-like. The phenomenology of such potentially large 3H self-interactions has been actively investigated at  $e^+e^-$  linear colliders within a manifold of processes, and compared to their counterpart processes in the MSSM. These analyses include e.g. the tree-level production of triple Higgs-boson final states [19]; the double Higgs-strahlung channels  $hhZ^0$  [20]; and the inclusive Higgs-pair production via gauge-boson fusion [21]. Also their fingerprint at the quantum level, in the form of large quantum effects, has been comprehensively reported in [14, 15]. All the abovementioned dynamical features also play a sensible role in the structure of the  $\gamma\gamma H$  coupling, as we shall see hereafter, and could not only entail hints of non-standard Higgs boson physics, but also a handle on the SUSY versus non-SUSY nature of a possible extended Higgs sector.

Our study of the process  $\gamma\gamma \rightarrow h$  is accomplished in correspondence with the most stringent experimental and theoretical constraints that restrict the allowed regions in the 2HDM and the MSSM parameter spaces. They stem fundamentally from the requirements of perturbativity, unitarity and vacuum stability, as well as from the EW precision data, the low-energy flavor-physics inputs and the Higgs mass regions ruled out by the LEP and Tevatron direct searches. Several studies in the literature provide a dedicated account on these topics [22, 23]. A more detailed description of the role of these constraints in the context of our analysis may be found e.g. in Ref. [14]. Let us stress, in particular, the critical role of perturbative unitarity, which enforces a limit on the strength of the Higgs self-interactions. In the present study we employ the most restrictive set of conditions proposed in Ref. [24] and discuss their impact with respect to the simplified approach that was first employed in our preliminary study of Ref. [10]. Tight bounds also follow from the radiative  $B$ -meson decay ( $b \rightarrow s\gamma$ ), as well as from the  $B_d^0 - \bar{B}_d^0$  mixing (which was not considered in [10]). While the former basically defines a lower bound on the charged Higgs mass  $M_{H^\pm} \gtrsim 300$  GeV for  $\tan\beta \geq 1$  [22] (which only applies to type-II 2HDM, but not to type-I), the latter strongly disfavors the regions of  $\tan\beta \lesssim 1$ , for both type-I and type-II 2HDM and, in general, tends to enforce  $\tan\beta \gtrsim 2$  for light charged Higgs bosons (viz.  $M_{H^\pm} \sim 100 - 150$  GeV) [23]. In our actual calculation we have included a fairly exhaustive collection of constraints by combining the packages *2HDMCalc* [25], *SuperISO* [23] and *HiggsBounds* [26], altogether with several complementary in-house routines. As for the algebraic calculation of the  $\gamma\gamma \rightarrow h$  cross-section, we have made use of the standard computational software

---

<sup>2</sup>We refer the reader to Ref. [14] for full details on the model setup, notation, definitions and various constraints.

2HDM	$M_{h^0}$ (GeV)	$M_{H^0}$ (GeV)	$M_{A^0}$ (GeV)	$M_{H^\pm}$ (GeV)
Set I	115	165	100	105
Set II	200	250	290	300

Table 1: Sets of 2HDM Higgs boson masses used throughout the calculation. Owing to the  $\mathcal{B}(b \rightarrow s\gamma)$  constraints on  $M_{H^\pm}$  [30], Set I is only possible for type-I 2HDM's, whereas Set II is possible for both type-I and type-II. The mass sets are enforced to satisfy the custodial symmetry bound  $|\delta\rho| < 10^{-3}$  – cf. Ref. [14].

*FeynArts*, *FormCalc* and *LoopTools* [27]. The Photon Luminosity functions, which account for the effective  $e^\pm \rightarrow \gamma$  “conversion” of the primary linac beam, are taken from the package *CompAZ* [28].

### 3 Numerical analysis

We shall next provide the main numerical results. For lack of space, in this Letter we cannot furnish analytical expressions for the calculation of the corresponding cross-sections. For explicit details, in particular for the complete set of Feynman diagrams and for the formulae that relate the basic “partonic”  $\sigma(\gamma\gamma \rightarrow h)$  cross-section to the the total averaged  $\gamma\gamma$  cross-section  $\langle\sigma_{\gamma\gamma \rightarrow h}\rangle(s)$  (unpolarized and convoluted with the differential luminosity distribution) as a function of the linac center of mass energy  $\sqrt{s}$ , we refer again the reader to our previous study of Ref. [10]. Furthermore, a detailed exposition of all the relevant pieces of the 2HDM interaction Lagrangian is given e.g. in our notation in [14]. The MSSM interactions are summarized e.g. in [3].

#### 3.1 $\gamma\gamma \rightarrow h$ within the 2HDM

Let us begin by revisiting the behavior of the total averaged cross-section  $\langle\sigma_{\gamma\gamma \rightarrow h}\rangle(s)$ , as well as of the relative strength of the effective  $\gamma\gamma h$  interaction normalized to the SM,  $r \equiv g_{\gamma\gamma h}/g_{\gamma\gamma H}^{\text{SM}}$ , in the framework of the 2HDM. In this context, the  $\gamma\gamma h$  effective vertex is generated at the quantum level through a rather complicated numerical interplay of the contributions from fermion,  $W^\pm$ -boson and charged Higgs boson loops, which include the trilinear self-interactions  $h^0 H^+ H^-$  and  $H^0 H^+ H^-$  – see Fig. 2 of Ref. [10]. In the MSSM case, we additionally have the squark and slepton loop contributions. Already from the dynamics of the  $\gamma\gamma h$  coupling in the SM, we know that the contribution of the (transverse components of the) gauge bosons are large and of opposite sign to the fermion and the scalar (namely the Goldstone boson) loops [29]. The very same interference pattern occurs in the 2HDM, and causes the phenomenological features to be critically sensitive to the charged Higgs boson couplings.

In Figures 1-2 we display the evolution of the total averaged single Higgs boson cross-section  $\langle\sigma_{\gamma\gamma \rightarrow h}\rangle(s)$  at a linac center of mass energy of  $\sqrt{s} = 500$  GeV, as a function of  $\sin\alpha$  and  $\tan\beta$  respectively. Notice that while in Fig. 1 we dwell on Set I of Higgs boson masses (cf. Table 1) and compare the cases  $\lambda_5 = 0$  and  $\lambda_5 = 1$ , in Fig. 2 we use both Higgs boson mass sets (I and II in Table 1), but concentrate on the setting  $\lambda_5 = 0$  only. In focusing on the latter case, we place ourselves in a scenario in which the overall size of the relevant 3H self-interactions is modulated solely by the actual  $\sin\alpha$  and  $\tan\beta$  values, along with the Higgs boson masses<sup>3</sup>. Our moderate choices of  $\lambda_5$  are motivated by the most restrictive set of unitarity constraints that we are using here [24]. These constraints no longer allow  $\lambda_5$  values as large as  $|\lambda_5| \gtrsim 10$ , for which the trilinear effects are very conspicuous, in fact the leading ones [10]. Here we will not consider the large  $\lambda_5$  scenario anymore, and we shall instead focus on mild values of order  $|\lambda_5| = \mathcal{O}(1)$ , which fall well within the regions permitted by unitarity. An example is the case  $\lambda_5 = 1$  studied in Fig. 1. It is

<sup>3</sup>For a detailed list of trilinear self-Higgs boson vertices in the general 2HDM, see e.g. Table II of Ref. [14].

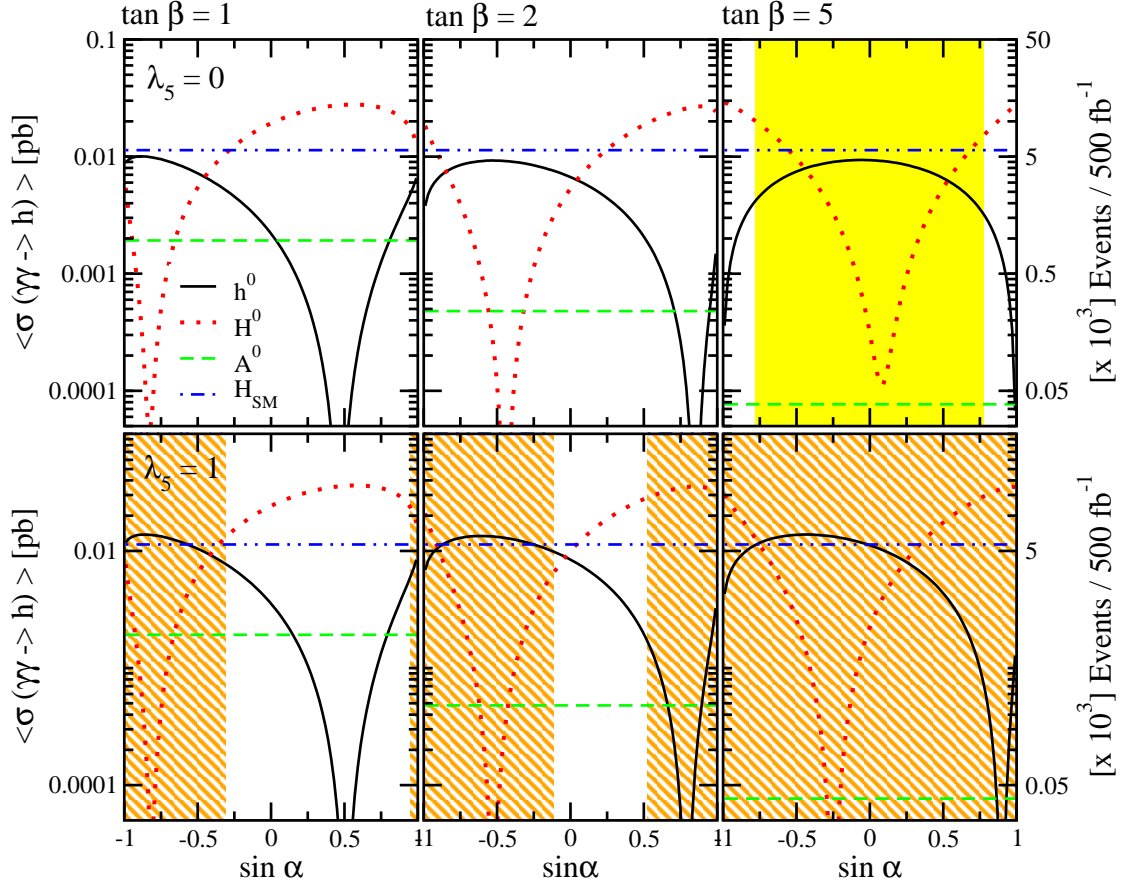


Figure 1: Total averaged cross-section  $\langle \sigma_{\gamma\gamma \rightarrow h^0} \rangle(s)$  for  $\sqrt{s} = 500$  GeV, and number of Higgs boson events, as a function of  $\sin \alpha$ . (Although the  $\mathcal{CP}$ -odd production channel  $\gamma\gamma \rightarrow A^0$  does not depend on this parameter, it is included for completeness.) Shown are the resulting cross-sections for the SM (dash-dotted horizontal line at  $\sigma_{SM} \simeq 0.011$  pb for  $M_{H_{SM}} = 115$  GeV), and the corresponding 2HDM ones for Higgs boson masses as in Set I, for  $\lambda_5 = 0$  (top panels) and  $\lambda_5 = 1$  (bottom panels), and for three values of  $\tan \beta$ . Notice that the characteristic suppression of the Higgs production rate (which takes place at different regions in the parameter  $\sin \alpha$  for each  $\mathcal{CP}$ -even channel) is a signature of the complementarity of the  $h^0 H^+ H^-$  and  $H^0 H^+ H^-$  self-couplings (cf. Table II of Ref. [14]). The shaded (yellow) area in the  $\tan \beta = 5$  case is excluded by unitarity, while the dashed (orange) regions in the bottom panels are disallowed by the vacuum stability conditions. Let us also underline that the  $\tan \beta = 1$  case is included to better assess the dependence of the cross section as a function of this variable, although the constraints stemming from  $B_d^0 - \bar{B}_d^0$  exclude it (see the text and the left panel of Fig. 3).

worthwhile stressing that, for moderate values  $|\lambda_5| \gtrsim 1$ , we meet in general a peculiar situation whereby the contribution from the trilinear coupling attains just the critical size which is able to partly counterbalance the rest of the quantum effects (viz. the loop effects triggered by the gauge bosons and the fermions with enhanced Yukawa couplings); and as a result we encounter a destructive interference scenario in most of the parameter space of the 2HDM. Let us recall, too, that the  $\lambda_5 > 0$  regions tend to be disfavored by the vacuum stability conditions – which become even more restrictive with growing values of  $\tan \beta$  (cf. the excluded areas in the lower panels of Fig. 1). Remarkably enough, even within this more restricted context we find very significant potential sources of new Higgs boson physics. In particular, the size of the cross-sections stays well within the measurable range and exhibits trademark phenomenological features, as we shall analyze in what follows.

Within this setup, Figs. 1-2 illustrate the results for the light ( $h^0$ ) and the heavy ( $H^0$ ) neutral

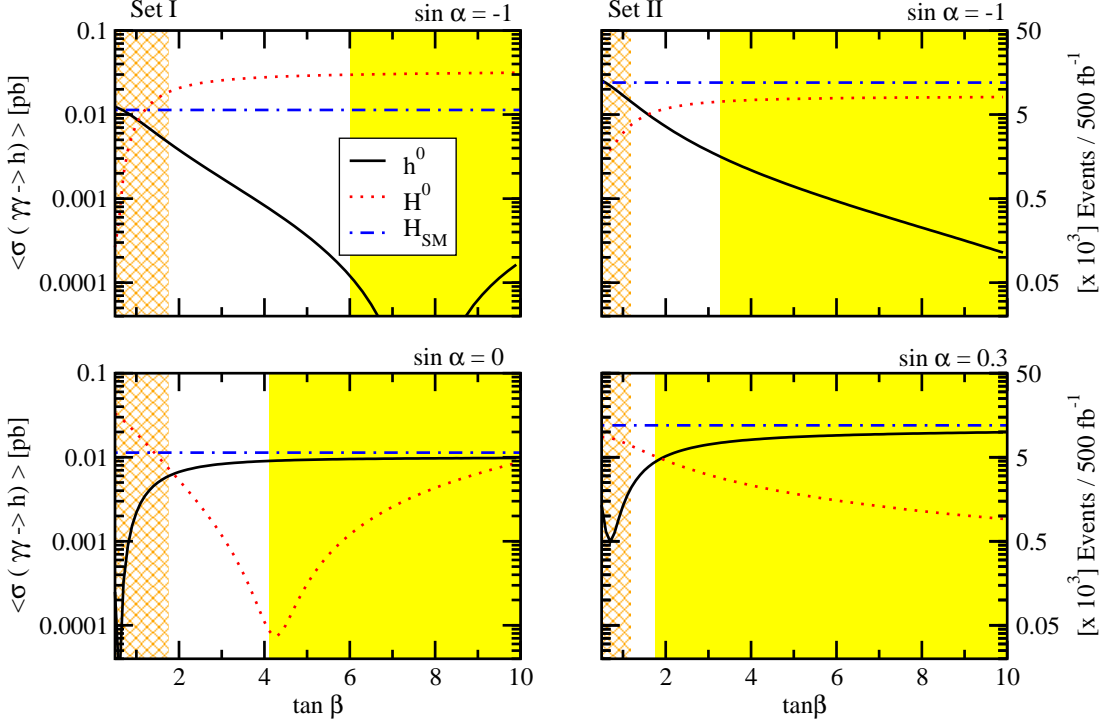


Figure 2: Cross-section  $\langle \sigma_{\gamma\gamma \rightarrow h^0} \rangle(s)$  ( $\sqrt{s} = 500$  GeV) and number of Higgs boson events, as a function of  $\tan\beta$ . We plot the  $\mathcal{CP}$ -even channels only, and compare the resulting cross-sections for the SM and the 2HDM by fixing the remaining Higgs boson masses as in Sets I and II, for  $\lambda_5 = 0$  and different choices of  $\sin\alpha$  (as indicated in the figure). The excluded  $\tan\beta$  range due to unitarity (yellow shaded area) and  $B_d^0 - \bar{B}_d^0$  mixing (orange crossed area) are explicitly indicated.

$\mathcal{CP}$ -even Higgs bosons, including also the  $\mathcal{CP}$ -odd state ( $A^0$ ), and compare the obtained rates from the 2HDM with the SM prediction for  $M_{H_{SM}} = M_{h^0}$ . From these plots we can easily read off the following relevant facts: i) the maximum cross sections may render  $\sigma = \mathcal{O}(10^{-2})$  pb; ii) the optimal  $h^0$  and  $H^0$  event rates are largely complementary to each other, as a result of the inverse correlation of the respective self-interactions  $h^0 H^+ H^-$  and  $H^0 H^+ H^-$  (once more we refer to Table II of Ref. [14]), which trigger the large suppressions (“dips” confronted with “cusps”) visible in the plots (e.g. quite notably in Fig. 1). We recall that their origin can be traced back to the destructive interference operating between the fermion, gauge boson and charged Higgs-mediated one-loop contributions to  $g_{h^0 \gamma \gamma}$ ; and iii) the maximum cross-section for the  $\mathcal{CP}$ -odd state  $A^0$  is significantly smaller than that of the  $\mathcal{CP}$ -even states (at least ten times smaller) but it does not get suppressed with  $\sin\alpha$ . For example, in the  $\tan\beta = 1$  case indicated in Fig. 1 it may lead to  $\sim 10^3$  events per 500 fb<sup>-1</sup> of integrated luminosity. For larger values of  $\tan\beta$ , however, the event rate decreases to the  $\sim 10^2$  level or below.

It is encouraging to see that, for the  $\mathcal{CP}$ -even states, the cross-sections can be quite sizeable away the suppressing dips in Figures 1-2, where they can render a few thousand events for  $h^0$ , and up to ten thousand events for  $H^0$ , per 500 fb<sup>-1</sup> of integrated luminosity. Admittedly in some cases the combination of unitarity and  $B_d^0 - \bar{B}_d^0$  mixing constraints enforces a relatively narrow region for the allowed parameter space, but in general it is still sufficiently large. Also remarkable is the fact that while the obtained rates for  $\gamma\gamma \rightarrow h^0$  tend to lie slightly below their SM counterparts, the  $\gamma\gamma \rightarrow H^0$  channel can have instead a cross-section larger than the SM case. This is a reflect of the behavior  $\sigma(\gamma\gamma \rightarrow h) \sim M_h^4/M_W^2$  in the general 2HDM, which implies that  $\sigma(H^0) > \sigma(H_{SM})$  since  $M_{H^0} > M_{H_{SM}} \equiv M_{h^0}$ .



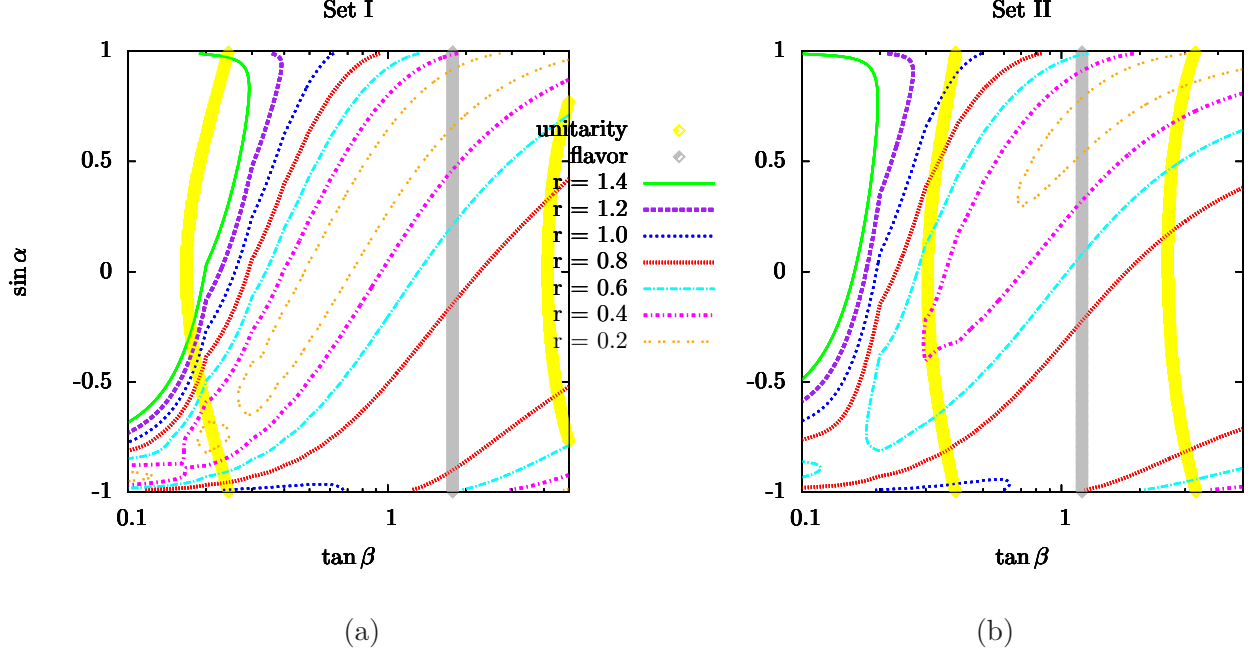


Figure 3: The ratio  $r \equiv g_{\gamma\gamma h^0}/g_{\gamma\gamma H}^{\text{SM}}$  measuring the effective  $\gamma\gamma h^0$  coupling strength in the 2HDM as compared to the SM, as a function of  $\sin \alpha$  and  $\tan \beta$ , for Sets I and II of Higgs boson masses in Table 1. The results have been obtained by setting  $\lambda_5 = 0$ . The yellow bands depict the lower and upper bounds on  $\tan \beta$ , out of which the restrictions of perturbative unitarity are violated. In turn, the grey band stands for the lower bound (at  $3\sigma$  C.L.) enforced by  $B_d^0 - \bar{B}_d^0$  mixing. The allowed region in the plots therefore is the one lying between the grey band and the rightmost yellow band.

How does the relative size of the 2HDM cross-sections versus the SM ones compare to the value of the ratio of the effective couplings  $\gamma\gamma h$  in both models, i.e.  $r = g_{\gamma\gamma h}/g_{\gamma\gamma H}^{\text{SM}}$ ? In Ref. [10] it was pointed out that, in the case of a type-I 2HDM, an enhancing effect up to  $r \simeq 4$  could be reached for relatively light charged Higgs bosons (as e.g. in Set I) and large enough 3H self-interactions – the optimal region being  $\lambda_5 \sim -20$  and  $\tan \beta \sim 1$ . As we have repeatedly emphasized, in the present analysis we adopt a more conservative perspective and hence stick to a specific, and more restrictive, set of unitarity constraints [24]. Their net effect is to pull down the maximum strength of the  $hH^+H^-$  ( $h = h^0, H^0$ ) self-coupling by a factor of roughly 4, meaning that the new maximally allowed values of the relative coupling strength are  $r \gtrsim 1$ . Figure 3 displays a detailed view on how  $r$  evolves in the  $(\tan \beta, \sin \alpha)$  plane, again under the assumption that  $\lambda_5 = 0$  and for the same Higgs boson mass sets. It is instructive to compare that figure with Fig. 5 (and Table 2) of Ref. [10], where we explored the influence of  $\lambda_5$  within a more relaxed set of unitarity conditions. The reduction by a factor of  $\sim 3 - 4$  becomes evident.

At first sight, one would expect that such reduction should translate into a depletion of the maximum cross sections by a factor roughly of  $r^2 \sim 10 - 20$ . In practice, however, the suppression turns out to be larger as a consequence of the aforementioned interference between the charged Higgs boson, fermion and gauge boson-mediated one-loop diagrams. Consequently, the potentially distinctive imprint of type-I 2HDM, in the form of a boost (up to a factor 10) with respect to the SM predictions fades away if we apply the more restrictive set of unitarity conditions, as we do in the present study. Fortunately, other distinctive phenomenological signatures may come into play.

Indeed, the relevant phenomenological signs may reside in the parameter region in which the combination of non-standard gauge/Yukawa couplings of the 2HDM stamp a fingerprint on the Higgs boson production cross section, therefore far from the regions where the triple Higgs self-

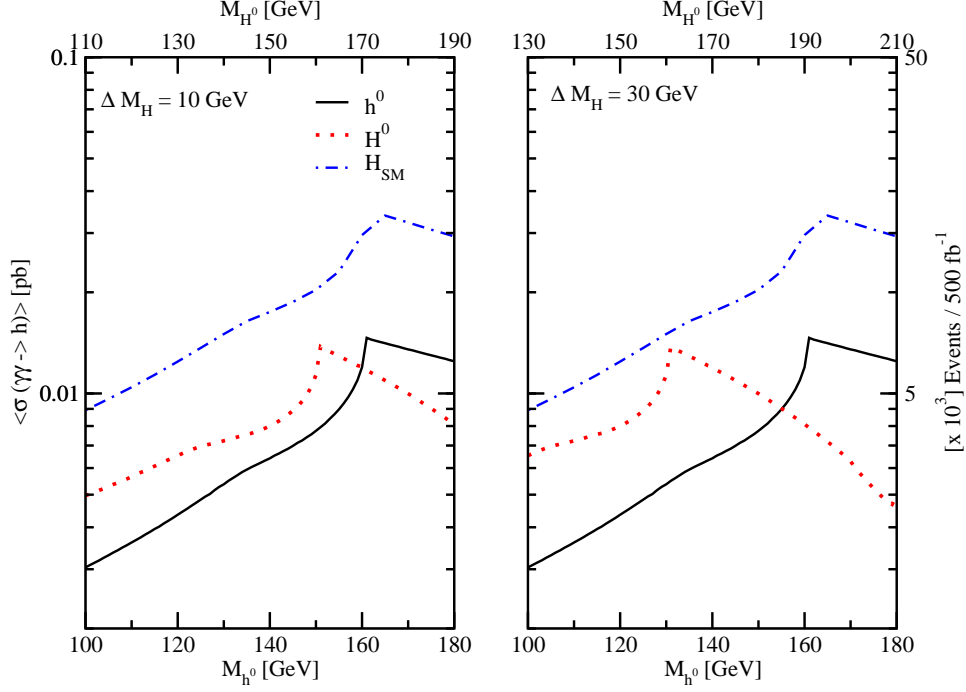


Figure 4: Total cross-section  $\langle \sigma_{\gamma\gamma \rightarrow h} \rangle(s)$  for  $\sqrt{s} = 500$  GeV and number of Higgs boson events, as a function of the CP-even Higgs boson masses ( $M_{h^0}$ , in the lower X-axis, and  $M_{H^0}$ , in the upper X-axis). The mass splitting between the two states is kept at 10 GeV (left panel) and 30 GeV (right panel). The Higgs boson masses are as in Set I, and for  $\sin \alpha = 0.30$ ,  $\tan \beta = 2$  and  $\lambda_5 = 0$ . The SM cross-section is also included (dash-dotted blue line). Remarkably, the two  $\mathcal{CP}$ -even states (solid and dotted lines) could be simultaneously accessible in the general 2HDM.

interactions alone dominate the loop-induced  $\gamma\gamma h$  coupling. As we have seen, this implies low values of  $\lambda_5$  and  $\tan \beta$  for a certain range of  $\sin \alpha$ . Notice, first of all, the existence of rather wide regions of the parameter space for which the  $\gamma\gamma \rightarrow h$  cross-section departs from its SM counterpart ( $\sigma_{SM} \simeq 11$  fb for a SM Higgs mass of  $M_{H_{SM}} = 115$  GeV, as in Set I). These regions are characterized by a sizable reduction – at the level of  $-10\%$  to  $-60\%$  – of the loop-induced  $\gamma\gamma h^0$  interaction in most of the  $\sin \alpha - \tan \beta$  plane, again due to the destructive interference modulated by the Higgs boson self-coupling  $h^0 H^+ H^-$ . On the other hand, augmented contributions with respect to the SM value (i.e.  $r > 1$ ) are only possible, at least theoretically, within a very constrained range:  $\tan \beta \sim 0.2 - 0.3$  (already bordering the unitarity and perturbativity limit). Here  $r$  can reach  $\sim 1.1 - 1.4$  (entailing cross-sections up to 20% larger than the SM ones) driven by the Higgs-top Yukawa coupling, which evolves as  $\sim 1/\tan \beta$  and therefore becomes enhanced in that range. Unfortunately, this region of parameter space is essentially ruled out by the experimental constraints dictated by  $B_d^0 - \bar{B}_d^0$  mixing [23], which hold for all possible Higgs-fermion coupling patterns. (Actually, the  $3\sigma$  exclusion region extends up to values of  $\tan \beta \sim 2$  for light charged Higgs boson masses, as shown in Fig. 3a for Set I). A very similar picture is encountered for Set II (see Fig. 3b), although the unitarity constraints become now more stringent, due to the presence of heavier Higgs bosons. As a consequence, the allowed regions for which the effective  $\gamma\gamma H^0$  departs significantly from  $r = 1$  cover a smaller patch of the  $\tan \beta - \lambda_5$  parameter space. However, for Set II the lower bound on  $\tan \beta$  dictated by  $B_d^0 - \bar{B}_d^0$  mixing is smaller:  $\tan \beta \gtrsim 1$  (cf. Fig. 3b). Let us also point out that type-I and type-II models are essentially indistinguishable from this point of view. This is an indication that both the Higgs-top quark coupling and the Higgs couplings to the gauge bosons, which are the relevant interactions in this domain, are common for both types of models.



The upshot of our analysis so far is that the task of spotting a “tail of subleading effects” triggered by the non-SM “Yukawa-gauge” sector of the theory should be perfectly feasible. Even if it might not enable discerning the particular type of 2HDM, the missing number of events could be a vigorous hint of a smoking gun – namely, of Higgs boson physics beyond the SM. This is of course under the assumption that the overall Higgs production rates lie only moderately below the SM predictions. Should the depletion be much larger, the actual missing number of events might not be enough to disentangle the signal from the dominant background process  $\gamma\gamma \rightarrow b\bar{b}$ .

Finally, in Fig. 4 we illustrate a very interesting phenomenological situation that could be particularly representative of genuine 2HDM physics. We consider the simultaneous production of two  $\mathcal{CP}$ -even Higgs bosons with moderate mass splittings of  $\Delta M_H = 10$  GeV and  $\Delta M_H = 30$  GeV. We focus our study around a mass region that comprises the upper mass bound that applies on the lightest  $\mathcal{CP}$ -even Higgs boson  $h^0$  in the MSSM, i.e.  $M_{h^0}^{\max} \simeq 115 - 140$  GeV. The results show that it is perfectly possible to produce simultaneously the two  $\mathcal{CP}$ -even Higgs states with similar masses in the general 2HDM, and both with large event rates of order  $\sim 10^3$  for the usual integrated luminosity of  $500 \text{ fb}^{-1}$  – and for relatively light (as in Set I) or heavy (as in Set II) Higgs boson spectra alike. This situation is impossible to realize in the MSSM, and therefore it would be a very distinctive signature of non-supersymmetric Higgs boson physics in a photon collider. In the next subsection, we dwell on the MSSM case in more detail.

### 3.2 $\gamma\gamma \rightarrow h$ within the MSSM

In a similar vein, we briefly address now the single  $\gamma\gamma$  production of Higgs bosons in the MSSM. While the general 2HDM case was first studied only very recently [10], the MSSM process has received a lot more of attention [8, 9]. Here we revisit the supersymmetric process in order to better compare with our detailed account of the general 2HDM case. The bottom-line of the MSSM studies on this process can be summarized as follows: in the most favorable situations, the relative effective strength of the  $\gamma\gamma h$  vertex with respect to the SM can reach up to  $r \simeq \sqrt{2} \simeq 1.4$ . There are basically two conditions under which this enhancements could be implemented: i) a large mass splitting between the chiral components of the squarks, in particular the stops – one of them being as light as possible; and ii) a large Higgs-squark Yukawa-like coupling, which means, for the stop in particular, a large value of the trilinear coupling  $A_t$ . The foresaid mass splitting can essentially be traced back to the soft-SUSY breaking pattern in the squark mass sector which, following standard conventions, can be written in terms of the mass matrix

$$M_{\tilde{Q}}^2 = \begin{pmatrix} M_{\tilde{Q}L}^2 + m_f^2 + \cos 2\beta (T_3^{fL} - Q_f \sin^2 \theta_w) M_Z^2 & m_f M_{LR}^f \\ m_f M_{LR}^f & M_{\tilde{Q}R}^2 + m_f^2 + \cos 2\beta Q_f \sin^2 \theta_w M_Z^2 \end{pmatrix}, \quad (1)$$

where  $M_{\tilde{Q}L,R}$  denote the soft-SUSY breaking masses for the left-handed (resp. right-handed) squark fields; while the off-diagonal pieces correspond to  $M_{LR}^u = A_u - \mu \cot \beta$  and  $M_{LR}^d = A_d - \mu \tan \beta$ . If the mass splitting  $\Delta m_{\tilde{f}} = m_{\tilde{f}_1} - m_{\tilde{f}_2}$  between the two mass eigenvalues is significant, this generates an asymmetry in the loop contributions to  $\gamma\gamma \rightarrow h$  induced by each of the squark components and allows a neat overall yield with a strength comparable to the gauge boson and the fermion-mediated counterparts.

It is precisely this kind of effects that were reported in the original MSSM calculations for single Higgs boson production, cf. Ref. [8, 9]. The scenarios considered therein, however, become problematic when they are revisited in the light of the current constraints on the MSSM parameter space. The presence of light stops, combined with a rather large trilinear coupling  $A_t$ , induces sizable one-loop corrections to the light  $\mathcal{CP}$ -even Higgs boson mass  $M_{h^0}$ , which easily clash with the limits on the phenomenologically excluded mass regime. By a similar token, light stops tend to

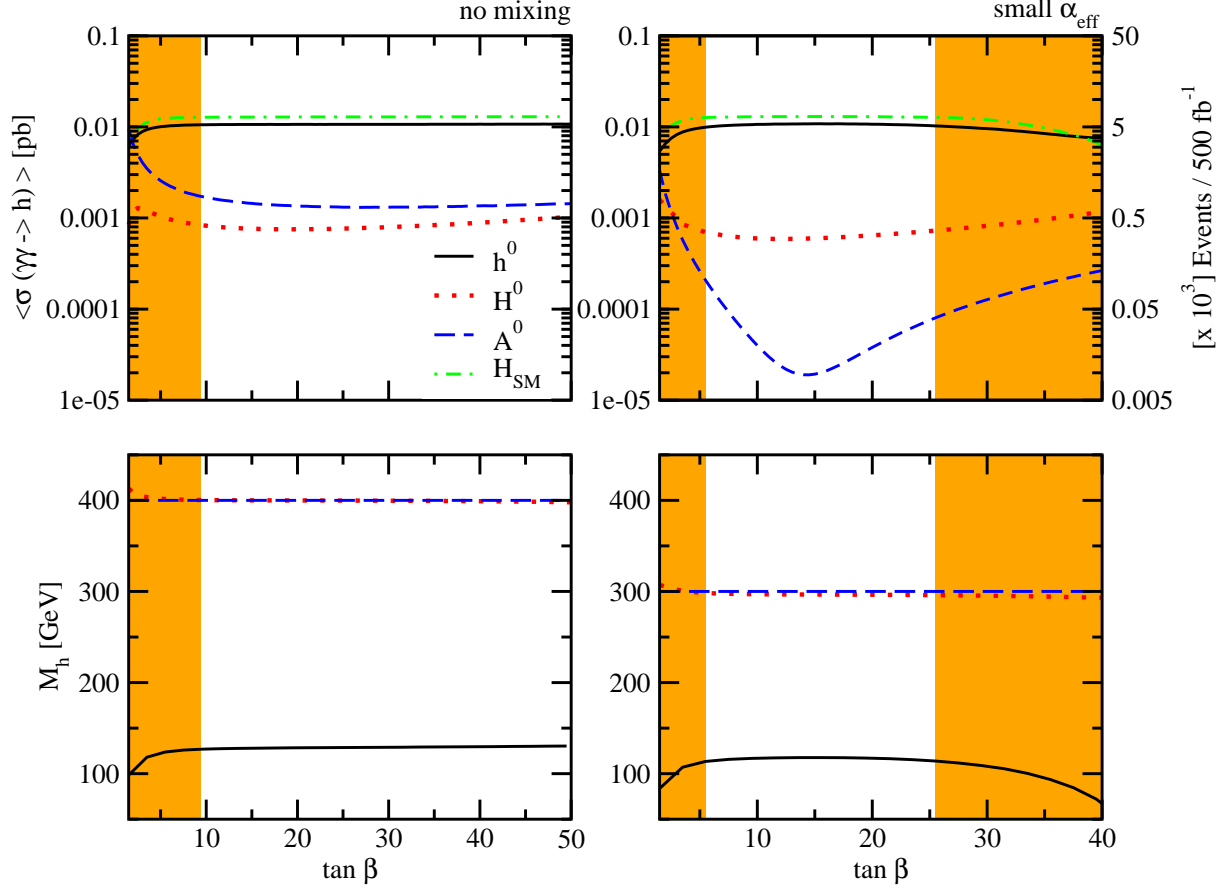


Figure 5: Cross-section  $\langle \sigma_{\gamma\gamma \rightarrow h^0} \rangle(s)$  and number of Higgs boson events as a function of  $\tan \beta$ . We plot the resulting cross-sections for the MSSM within the benchmark scenarios quoted in Table 2, and compare them to the SM. In the bottom panels we account for the the light (versus heavy) neutral  $\mathcal{CP}$ -even MSSM Higgs boson masses as a function of  $\tan \beta$ . The shaded bands stand for the excluded mass regimes. The center of mass energy is fixed at  $\sqrt{s} = 500$  GeV

be disfavored from either indirect restrictions (mainly from  $\mathcal{B}(b \rightarrow s\gamma)$  constraints [30]) and from the direct searches conducted at the Tevatron, and currently underway at the LHC [31]. To be sure, many of the theoretically best motivated realizations of SUSY tend to accommodate a squark spectrum with masses heavier than a few hundred GeV – this is indeed the reason why relatively heavy squarks are ubiquitous in the standard benchmark points defined in the literature (viz. the Les Houches [32] or the SPS convention [33]).

With these provisos in mind, let us now present the results of our own (fully updated) calculation of the single MSSM Higgs boson production at a photon collider,  $\gamma\gamma \rightarrow h$  ( $h = h^0, H^0, A^0$ ), by taking into account, in particular, the current mass bounds stemming from direct SUSY particle searches at the LEP and Tevatron [34], and most significantly the presently allowed Higgs boson mass range [26]. Further restrictions, such as the compliance with the limits imposed by  $\mathcal{B}(b \rightarrow s\gamma)$  [30] and  $B_d^0 - \bar{B}_d^0$  data [23], are also duly taken into account. Worthwhile mentioning is that, in contrast to the general 2HDM case, here we do not have severe unitarity bounds because the MSSM Higgs boson self-couplings are purely gauge. Even so, the predicted  $\gamma\gamma \rightarrow h^0$  rate in the MSSM is highly subdued by the remaining constraints and, overall, it appears rather mild, in the sense of being highly undifferentiated with respect to the SM case, whereas the signals for  $H^0$  and  $A^0$  production are usually much smaller. A panoramic view of the MSSM results is presented

scenario	no-mixing	Small $\alpha_{eff}$
$M_{A^0}$ (GeV)	400	300
$M_{SUSY}$ (GeV)	2000	800
$\mu$ (GeV)	200	2000
$X_t \equiv A_t - \mu/\tan\beta$ (GeV)	0	-1100
$M_2$ (GeV)	200	500
$M_3$ (GeV)	1600	500

Table 2: MSSM parameter settings corresponding to two benchmark scenarios, as defined in Ref. [32]. GUT relations between the electroweak gaugino soft SUSY-breaking masses, as well as universal trilinear couplings ( $A_t = A_b = A_\tau$ ), are assumed.

in Figs. 5 and 6.

Let us dwell on these Figures in more detail. For example, in Fig. 5 we survey the total MSSM single Higgs boson cross section  $\langle\sigma_{\gamma\gamma\rightarrow h^0}\rangle$  at fixed  $\sqrt{s} = 500\text{ GeV}$  as a function of  $\tan\beta$ , for two standard benchmark points (cf. Table 2), and we compare it to the SM yield – identifying  $M_{H_{SM}}$  with  $M_{h^0}$ . We have computed in Fig. 5 (bottom panels) the corresponding mass spectrum for the neutral,  $\mathcal{CP}$ -even states with the help of *FeynHiggs* [35]. The obtained cross sections for  $h^0$  lie very close, though slightly below, the SM expectations – similarly to the behavior exhibited by the 2HDM for those scenarios with small 3H self-couplings. This translates into few thousand event rates – few hundred for  $H^0$ , and even less for  $A^0$ . The profile of  $\langle\sigma_{\gamma\gamma\rightarrow h^0}\rangle$  as a function of  $\tan\beta$  is essentially featureless and is mostly correlated to the change in the Higgs boson mass. We also notice from the bottom panels of Fig. 5 that the mass splitting between the  $\mathcal{CP}$ -even Higgs bosons can never mimic the 2HDM situation previously illustrated in Fig. 4, in which these states could be simultaneously produced with similar cross-sections. Indeed, we see that in the MSSM case there is a suppression of the heavy  $\mathcal{CP}$ -even Higgs by roughly one order of magnitude because the behavior of the cross-section can never be enhanced by a moderately heavier Higgs boson mass, in contrast to the general 2HDM case. We point out that we have carried out the same analysis for the other benchmark points defined in Ref. [32] and found very similar phenomenological trends to those that characterize the *no-mixing* scenario, and so we will not report on these results in this Letter.

Let us note that we have called the “tail of subleading effects” in the 2HDM case is also the main source of the MSSM corrections and proceeds essentially through the same Yukawa, and Yukawa-like, couplings of the Higgs bosons with the quarks (here also with the squarks), although in this case the angles  $\alpha$  and  $\beta$  are of course tied by the SUSY relations [3]. Thus, in contrast to the 2HDM, the MSSM is unable to furnish a significant enhancement or suppression of the ratio  $r = g_{\gamma\gamma h}/g_{\gamma\gamma H}^{\text{SM}}$  (see Fig. 6, and compare it with Fig. 3), the reason being the absence of large 3H self-couplings, and hence the lack of a mechanism capable of prompting the characteristic interference pattern that we have singled out for the 2HDM. At the same time the additional, purely SUSY, contributions to  $g_{\gamma\gamma h}$ , namely the squark-mediated loops (whose enhancing capabilities originate in the Higgs-squark Yukawa couplings) turn out to be not so competitive, as they are pulled down by inverse powers of the SUSY-breaking mass scale, and further limited by the Higgs and squark mass bounds and the flavor physics restrictions. As a matter of fact, our updated calculation of  $r = g_{\gamma\gamma h}^{\text{MSSM}}/g_{\gamma\gamma H}^{\text{SM}}$  displays departures from  $r = 1$  which are typically milder than those reported in former analyses on the topic [8, 9]. Upon sweeping the MSSM parameter space, we confirm that the prominent regions documented in the old literature do exist theoretically, although they are no longer allowed in practice when all current phenomenological constraints are plugged into the analysis. In particular, the combination of the Higgs boson mass bounds and the

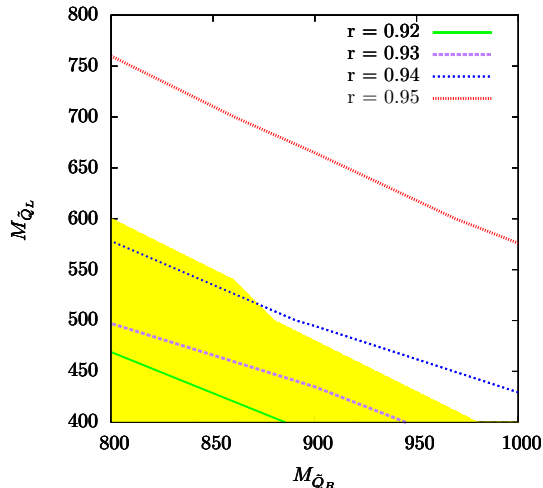


Figure 6: Ratio  $g_{h^0\gamma\gamma}/g_{H\gamma\gamma}$  in the  $M_{\tilde{Q}_L}$  -  $M_{\tilde{Q}_R}$  plane, cf. Eq. (1), in which the separate variation of the left- and right-handed squark soft SUSY-breaking masses gives rise to an explicit mixing in the squark chiral sector – see the text for details. The remaining MSSM parameters are set along as follows:  $\tan\beta = 2$ ,  $M_{A^0} = 600$  GeV,  $\mu = 500$  GeV,  $A_t = 1800$  GeV,  $M_2 = 500$  GeV. GUT relations between  $M_1$  and  $M_2$ , as well as universal trilinear couplings ( $A_t = A_b = A_\tau$ ), are assumed. The shaded region is ruled out by  $\mathcal{B}(b \rightarrow s\gamma)$ .

$\mathcal{B}(b \rightarrow s\gamma)$  restrictions turns out to cripple considerably the formerly reported enhancement power encompassed by the MSSM. This is what we aim at illustrating in Figure 6, where the evolution of the relative  $\gamma\gamma h^0$  coupling strength  $r$  is explored as a function of the left-to-right squark mass splitting. For a sizable Higgs-stop trilinear coupling  $A_t = 1800$  GeV, we single out deviations up to  $r \sim -5\%$ , which are correlated with the lightest attainable squark masses – and the maximum mass splitting between their chiral components. We conclude that the MSSM can only induce rather tempered quantum effects as compared to the 2HDM.

## 4 Discussion and conclusions

In this Letter, we have reported on a comparative study of the production of a single neutral Higgs boson,  $h = h^0, H^0, A^0$  both within the general two-Higgs-doublet model (2HDM) and in the Minimal Supersymmetric Standard Model (MSSM). Motivated by the robust handle on new physics that would represent a precise measurement of the effective  $\gamma\gamma h$  coupling at a photon collider, we have computed the single Higgs boson production cross sections  $\langle\sigma_{\gamma\gamma \rightarrow h^0}\rangle(s)$  in the aforementioned models and compared them to the SM results. In our study we have applied all known current restrictions on the parameter spaces of both models coming from unitarity, perturbativity, custodial symmetry and low-energy flavor physics. The typical values for the production cross-section of the lightest  $\mathcal{CP}$ -even state  $h^0$  at  $\sqrt{s} = 500$  GeV fall in the ballpark of  $\sigma \sim \mathcal{O}(10^{-2})$ pb in both the 2HDM and the MSSM. In contrast, while the heaviest  $\mathcal{CP}$ -even state ( $H^0$ ) can be produced with similar (even higher) rates in the 2HDM, its cross-section is roughly one order of magnitude depressed in the MSSM. The next relevant issue is to understand how the extra degrees of freedom and/or the non-standard dynamical features of either model, the 2HDM or the MSSM, may leave a significant imprint of the new physics, and whether they can give rise to distinctive signatures. The size of the 3H self-couplings plays a decisive role here. Depending on the strength of the self interactions between the charged and the neutral  $\mathcal{CP}$ -even Higgs bosons in the general 2HDM, one of the following three situations emerges:

1. Large  $\lambda_{hH^+H^-}$  self-coupling. If sufficiently enhanced (namely  $\lambda_{hH^+H^-} \gtrsim 10^3$  GeV), this coupling would induce a large contribution from the charged Higgs boson mediated loops that would overcome the combined (negative) quantum effects driven by the fermion and the gauge boson loops. This is the scenario originally exploited in Ref. [10], in which the size of the 3H self-couplings was boosted by a large value of  $|\lambda_5| \gtrsim 10$ . However, if one adopts a more conservative assumption for the unitarity bounds [24], this scenario becomes unfavored.
2. Moderate  $\lambda_{hH^+H^-}$  at the level of  $\mathcal{O}(10^2)$  GeV. These values are amply permitted by the more restrictive unitarity bounds [24] and yet produce a substantial (destructive) interference with the gauge boson and fermion mediated loops, thence pulling the expected single Higgs boson rates down to values below the SM expectations, although still perfectly measurable in many cases. Interestingly enough, both the scenarios 1) and 2) are theoretically very appealing, as they rely on a genuine dynamical feature of the 2HDM – namely the “Yukawa-like” nature of the Higgs boson self-interactions and their enhancing potential – which is unmatched in the MSSM.
3. Small  $\lambda_{hH^+H^-}$ , roughly of  $\mathcal{O}(10)$  GeV, such that the charged Higgs boson mediated corrections are relegated to a subleading level. In this case, one is basically left with the SM-like gauge and Yukawa contributions, with an additional modulation according to how quarks and gauge bosons couple to  $h = h^0, H^0, A^0$  in the 2HDM. These non-standard features translate numerically into  $r \equiv g_{\gamma\gamma h}/g_{\gamma\gamma h}^{\text{SM}} \lesssim 1$  – hence a rather mild depletion of the single Higgs boson rate with respect to the SM one. This situation shows a clear overlap with the typical picture that we have obtained for the MSSM, where one has, in addition, the Yukawa-like effects from the Higgs boson interactions with squarks. In such circumstance there is still a chance to discriminate the  $\gamma\gamma \rightarrow h$  signatures triggered by both models (2HDM and MSSM), most significantly through a possible correlation of the  $\gamma\gamma \rightarrow h^0$  and  $\gamma\gamma \rightarrow H^0$  processes. Indeed, as SUSY enforces a relatively large mass splitting between  $h^0$  and  $H^0$  (cf. bottom panels of Fig. 5), it would be unable to account for a scenario such as the one addressed in Fig. 4, in which the two  $\mathcal{CP}$ -even Higgs bosons are produced at similar sizeable rates. Such situation would manifest through the detection of two back-to-back  $b$ -jets pointing to two different scalar resonances whose mass separation could possibly be resolved by the attainable sensitivity in the dijet invariant mass reconstruction <sup>4</sup>. A signature of this sort would undoubtedly provide a very strong hint of (non-SUSY) Higgs physics beyond the SM. In practice, of course, this statement holds only if we assume a situation similar to that of Fig. 2, in which we spotlight regions where both  $h^0$  and  $H^0$  are produced at a rate of order  $1 - 10$  fb, namely regions where neither the  $h^0H^+H^-$  nor the  $H^0H^+H^-$  self-interactions are large enough to sharpen the destructive interference with the gauge and fermion-mediated loop corrections.

A few concluding remarks are in order. On the face of the typical single Higgs boson rates emerging from direct  $\gamma\gamma \rightarrow h$  scattering, which lie in the ballpark of a few thousand events per  $500 \text{ fb}^{-1}$  of integrated luminosity (for a center-of-mass energy range of  $\sqrt{s} = 500 - 1000 \text{ GeV}$ ), it is pretty obvious that the prospects for Higgs boson detection in a  $\gamma\gamma$ -collider are quite encouraging. To start with, let us stress that the single Higgs-boson final state is to be produced essentially at rest. Therefore, for  $M_h < 2M_W \lesssim 160 \text{ GeV}$ , the corresponding signatures should mostly be in the form of back-to-back, highly energetic, quark jets ( $b\bar{b}$ ,  $c\bar{c}$ ). For  $M_h > 2M_W$  and specially for  $M_h > 2M_Z \simeq 180 \text{ GeV}$ , instead, signatures with two or four charged leptons in the final state

---

<sup>4</sup>A rough estimate of this sensitivity provides  $\Delta M \sim 2 \text{ GeV}$  [9], although a much better mass resolution should be in principle reachable at a photon collider, cf. e.g. [36].

(from  $W^\pm \rightarrow \ell^\pm + \text{missing energy}$  and, particularly, from  $Z \rightarrow \ell^+\ell^-$ ) should be crystal-clear. To these signatures we should add the radiative decay  $h \rightarrow \gamma\gamma$ , which will be at work with the same dynamics as the production  $\gamma\gamma \rightarrow h$  mechanism. Although its branching ratio is generally small ( $\lesssim 10^{-3}$ ), it could be enhanced significantly in the 2HDM case [12]. With enough statistics on these various signatures and from the analysis of the invariant mass distribution of the resulting dijet and dilepton-track signatures, the measurement of the Higgs boson mass(es) should be attainable with fairly good accuracy, together with a precise determination of the effective  $g_{\gamma\gamma h}$  couplings (typically for  $h^0$ , and most likely also for  $H^0$  in the 2HDM).

The new results reported here, despite being based on scenarios markedly different from the ones emphasized in our previous study [10], keep on spotlighting the excellent opportunities offered by direct  $\gamma\gamma$  collisions at future linac facilities, in particular in the domain of high precision Higgs boson experiments. After having produced one or more Higgs bosons, an accurate determination of the effective coupling(s)  $g_{\gamma\gamma h}$  might not only carry undisputed evidence of a non-standard Higgs boson dynamics, but also a distinctive signature of its fundamental supersymmetric or non-supersymmetric origin. In the MSSM case, since  $r = g_{\gamma\gamma h^0}/g_{\gamma\gamma H}^{\text{SM}}$  is expected to be rather close to 1 it would be necessary to measure the presence of additional Higgs states. Fortunately, the SUSY  $\gamma\gamma \rightarrow h$  yield, even if it became now much more subdued (comparatively to previous studies [8,9]), is still sizeable. The main mode is the light  $\mathcal{CP}$ -even state  $h^0$ , which can be produced with cross-sections that amount to a few thousand events per  $500\text{fb}^{-1}$  of integrated luminosity, whereas the heavy  $\mathcal{CP}$ -even state  $H^0$  (and in some cases the  $\mathcal{CP}$ -odd one,  $A^0$ , as well) can still render a few hundred events. This shows that a photon-photon collider could help decisively in escaping the “cul de sac” kind of situation in which MSSM Higgs boson physics might end up at the LHC if the physical parameter space lies in the infamous (so-called) “LHC wedge” [2], namely that region characterized by  $M_{A^0} > 200$  GeV and intermediate values of  $\tan\beta$ . Should Higgs boson events potentially detected at the LHC fall in this “trap” of the MSSM parameter space, one could not obviously decide about the nature of the produced single Higgs boson, as the light supersymmetric  $\mathcal{CP}$ -even state  $h^0$  would then be nearly indistinguishable from the SM Higgs boson (and at the same time the heavy Higgs bosons would be virtually undetectable at the LHC there). Remarkably enough, the MSSM benchmark points we have used (cf. Table 2 and Fig. 5) are just in the LHC wedge region, showing that even in this unfavorable circumstance for the LHC at least two supersymmetric Higgs bosons could still be accessible to  $\gamma\gamma$  physics in the ILC. Clearly, the unique opportunity offered by a photon-photon collider for a simultaneous measurement of additional Higgs bosons, with smaller or similar rates to the  $h^0$  one, would suggest new physics of SUSY or non-SUSY nature respectively.

**Acknowledgments** The work of JS has been supported in part by DIUE/CUR Generalitat de Catalunya under project 2009SGR502; by MEC and FEDER under project FPA2010-20807. This work was also partially supported by the Spanish Consolider-Ingenio 2010 program CPAN CSD2007-00042.

## References

- [1] P.W. Higgs, *Phys. Lett.* **12** (1964) 32; *Phys. Rev. Lett.* **13** (1964) 508; F. Englert and R. Brout, *Phys. Rev. Lett.* **13** (1964) 321; G.S. Guralnik, C.R. Hagen and T. W. B. Kibble, *Phys. Rev. Lett.* **13** (1964) 585.
- [2] H. Haber, *Present status and Future prospects for a Higgs boson discovery at the Tevatron and the LHC*, *J. Phys. Conf. Ser.* **G259** (2010) 012017, arXiv:1011.1038 [hep-ph].



- [3] J.F. Gunion, H.E. Haber, G.L. Kane and S. Dawson, *The Higgs hunter's guide*, Addison-Wesley, Menlo-Park, 1990.
- [4] G. C. Branco *et al.*, *Theory and phenomenology of two-Higgs-doublet models*, arXiv:1106.0034.
- [5] A. Djouadi, *Phys. Rept.* **457** (2008) 1; *Phys. Rept.* **459** (2008) 1; S. Heinemeyer, W. Hollik, G. Weiglein, *Phys. Rept.* **425** (2006) 265; S. Heinemeyer, *Acta Phys. Polon.* **B39** (2008) 2673, arXiv:0807.2514 [hep-ph].
- [6] *ILC Reference Design Report Volume 2: Physics at the ILC*, arXiv:0709.1893 [hep-ph]; *Physics interplay of the LHC and the ILC*, (G. Weiglein *et al.*), *Phys. Rept.* **426** (2006) 47.
- [7] See e.g. V. I. Telnov, *Nucl. Phys. Proc. Supp.* **184** (2008) 271; *Acta Phys. Pol.* **B 37** (2006) 1049; A. de Roeck, *Nucl. Phys. Proc. Supp.* **179-180** (2008) 94-103; B. Badelek *et al.*, *Int. J. of Mod. Phys.* **A 19** (2004) 5097.
- [8] B. Grzadkowski, J.F. Gunion, *Phys. Lett.* **B294** (1992) 361; J. F. Gunion, H.E. Haber, *Phys. Rev.* **D48** (1993) 5190; D.L. Borden, D.A. Bauer, D.O. Caldwell, *Phys. Rev.* **D48** (1993) 4018; M. Mühlleitner, M. Krämer, M. Spira, P. Zerwas, *Phys. Lett.* **B508** (2001) 311; D. M. Asner, J. B. Gronberg, J.F. Gunion, *Phys. Rev.* **D67** (2003) 035009; P. Niezurawski, A.F. Zarnecki and M. Krawczyk, *Acta Phys. Polon.* **B 37** (2006) 1187.
- [9] S-h. Zhu, C-s. Li, C-s. Gao, *Chin. Phys. Lett.* **15** (1998) 89; M. Krawczyk, *Photon photon and electron photon physics or physics at photon collider*, arXiv:hep-ph/0307314.
- [10] N. Bernal, D. López-Val and J. Solà, *Phys. Lett.* **B677** (2009) 38, arXiv:0903.4978 [hep-ph].
- [11] F. Cornet and W. Hollik, *Phys. Lett.* **B669** (2008) 58; E. Asakawa, D. Harada, S. Kanemura, Y. Okada and K. Tsumura, *Phys. Lett.* **B672** (2009) 354; A. Arhrib, R. Benbrik, C.-H. Chen, and R. Santos, *Phys. Rev.* **D80** (2009) 015010; E. Asakawa, D. Harada, S. Kanemura, Y. Okada, K. Tsumura, *Phys. Rev.* **D82** (2010) 115002, arXiv:1009.4670;
- [12] P. Posch, *Phys. Lett.* **B696** (2011) 447, arXiv:1001.1759 [hep-ph]; D. Phalen, B. Thomas, J. D. Wells, *Phys. Rev.* **D75** (2007) 117702, hep-ph/0612219; A. Arhrib, W. Hollik, S. Peñaranda, M. Capdequi Peyranère, *Phys. Lett.* **B579** (2004) 361; hep-ph/0307391; I. F. Ginzburg, M. Krawczyk, P. Osland, *Nucl.Instrum.Meth.* **A472** (2001) 149, hep-ph/0101229.
- [13] J.A. Coarasa, D. Garcia, J. Guasch, R.A. Jiménez, J. Solà, *Eur. Phys. J* **C2** (1998) 373, arXiv:hep-ph/9607485; *Phys. Lett.* **B425** (1998) 329, arXiv:hep-ph/9711472; D. Garcia, W. Hollik, R.A. Jiménez, J. Solà, *Nucl. Phys.* **B427** (1994) 53, arXiv:hep-ph/9402341; S. Béjar, J. Guasch, D. López-Val, J. Solà, *Phys. Lett.* **B668** (2008) 364, arXiv:0805.0973 [hep-ph], and references therein.
- [14] D. López-Val and J. Solà, *Phys. Rev.* **D81** (2010) 033003, arXiv:0908.2898 [hep-ph]; D. López-Val and J. Solà, *PoS RADCOR2009*, 045 (2010), arXiv:1001.0473 [hep-ph].
- [15] D. López-Val, J. Solà and N. Bernal, *Phys. Rev.* **D81** (2010) 113005, arXiv:1003.4312 [hep-ph]; J. Solà and D. López-Val, *Fortsch. Phys.* **G58** (2010) 660.
- [16] M. Moretti, F. Piccinini, R. Pittau, J. Rathsmann, *JHEP* 1011 (097) 2010, arXiv:1008.0820; S. S. Bao, Y. L. Wu, *Phys. Rev.* **D81** (2010) 075020, arXiv:0907.3606 [hep-ph].
- [17] J. A. Coarasa, J. Guasch, J. Solà and W. Hollik, *Phys. Lett.* **B442** (1998) 326, hep-ph/9808278.

- [18] A. Pich, P. Tuzón, *Phys. Rev.* **D80** (2009) 091702, arXiv:0908.1554; A. Buras, M. V. Carlucci, S. Gori, G. Isidori, *JHEP* 1010 (2010) 009, arXiv:1005.5310 [hep-ph]; M. Aoki, S. Kanemura, K. Tsumura, K. Yagyu, *Phys. Rev.* **D80** (2009) 015017, arXiv:0902.4665 [hep-ph].
- [19] G. Ferrera, J. Guasch, D. López-Val and J. Solà, *Phys. Lett.* **B659** (2008) 297, arXiv:0707.3162 [hep-ph]; PoS RADCOR2007, 043 (2007), arXiv:0801.2469 [hep-ph].
- [20] A. Arhrib, R. Benbrik and C.-W. Chiang, *Phys. Rev.* **D77** (2008) 115013, arXiv:0802.0319 [hep-ph]; AIP Conf.Proc.1006, 112 (2008).
- [21] R. N. Hodgkinson, D. López-Val and J. Solà, *Phys. Lett.* **B673** (2009) 47, arXiv:0901.2257 [hep-ph].
- [22] A. Wahab El Kaffas, P. Osland, O. M. Greid, *Phys. Rev.* **D76** (2007) 095001, arXiv:0706.2997; H. Flücher, M. Goebel, J. Haller, A. Höcker, K. Mönig, J. Stelzer, *Eur. Phys. J* **C60** (2009) 543, arXiv:0811.0009; N. Mahmoudi, O. Stal, *Phys. Rev.* **D81** (2010) 035016, arXiv:0907.1791 [hep-ph].
- [23] F. Mahmoudi, *Com. Phys. Comm.* **G178** (2008) 745, arXiv:0710.2067 [hep-ph]; *Com. Phys. Comm.* **G180** (2009) 1579, arXiv:0808.3144 [hep-ph]; <http://superiso.in2p3.fr>.
- [24] S. Kanemura, T. Kubota and E. Takasugi, *Phys. Lett.* **B313** (1993) 155; A. Akeroyd, A. Arhrib, E.-M. Naimi, *Phys. Lett.* **B490** (2000) 119, arXiv:hep-ph/0006035. See also Sect. III of Ref. [14].
- [25] D. Eriksson, J. Rathsman, O. Stal, *Com. Phys. Comm.* **G181** (2010) 189, arXiv:0902.0851; <http://www.isv.uu.se/thep/MC/2HDMC/>.
- [26] P. Bechtle, O. Brein, S. Heinemeyer, G. Weiglein, K. E. Williams, *Com. Phys. Comm.* **G181** (2010) 138, arXiv:0811.4169, arXiv:1102.1898; <http://www.ippp.dur.ac.uk/HiggsBounds>.
- [27] T. Hahn, *FeynArts 3.2*, *FormCalc* and *LoopTools* user's guides, available from <http://www.feynarts.de>; T. Hahn, *Comput. Phys. Commun.* **168** (2005) 78.
- [28] V. I. Telnov, *Acta Phys. Polon.* **B 37** (2006) 633; A. F. Zarnecki, *Acta Phys. Polon.* **B34** (2003) 2741.
- [29] J. Ellis, M. K. Gaillard, D. V. Nanopoulos, *Nucl. Phys.* **B106** (1976) 292.
- [30] M. Misiak *et al.* *Phys. Rev. Lett.* **98** (2007) 022002.
- [31] The CMS Collaboration, *Phys. Lett.* **B698** (2011) 196, arXiv:1101.1628 [hep-ex].
- [32] M. S. Carena, S. Heinemeyer and C. E. M. Wagner, *Eur. Phys. J* **C26** (2003) 601, arXiv:hep-ph/0202167.
- [33] B. C. Allanach *et al.*, *Eur. Phys. J* **C25** (2002) 113, arXiv:hep-ph/0202233.
- [34] K. Nakamura *et al.* (Particle Data Group), *J. Phys.* **G37** (2010) 075021.
- [35] S. Heinemeyer, W. Hollik and G. Weiglein, *Com. Phys. Comm.* **G124** (2000) 76, arXiv:hep-ph/9812320; S. Heinemeyer, W. Hollik and G. Weiglein, *Eur. Phys. J* **C9** (1999) 343, arXiv:hep-ph/9812472; G. Degrandi, S. Heinemeyer, W. Hollik and P. Slavich, *Eur. Phys. J* **C28** (2003) 133, arXiv:hep-ph/0212020; M. Frank *et al.*, *JHEP* 02 ((2007)) 047, arXiv:hep-ph/0611326.
- [36] A. de Roeck, *Nucl. Phys. Proc. Supp.* **126** (2004) 386-395.